2007

Performance Modeling of an RF Coaxial Plasma Thruster

William B. Stein
Purdue University

Alina A. Alexeenko
Purdue University - Main Campus, alexeenk@purdue.edu

Ivana Hrbud
Purdue University

Evgeniy Bondar

43rd AIAA/ASME/SAE/ASEE Joint Propulsion Conference & Exhibit
8 - 11 July 2007, Cincinnati, OH

AIAA 2007-5292

2007-5292

Joint Propulsion Conference, 8-11 July 2007, Cincinnati, OH

Performance Modeling of an RF Coaxial Plasma Thruster

William B. Stein[*], Alina A. Alexeenko[†], and Ivana Hrbud[‡]
Purdue University, West Lafayette, IN 49707, U.S.A.

Evgeniy Bondar[§]
Khristianovich Institute of Theoretical and Applied Mechanics, Novosibirsk, 630090, Russia

The RF plasma thruster has considerable potential to ease the impact of severe constraints on power, mass, volume and lifetime of microsatellite propulsion systems. This concept is classified as an electrothermal propulsion system and exploits RF capacitively coupled discharge (RFCCD) for heating of a propellant. The plasma is characterized as a low-power discharge possessing a low-current density with high uniformity and propagating through low-pressure gas. To assess computationally the thruster's propulsive capabilities as a function of mass flow rate, electrode separation, RF frequency and power input, a numerical model comprises particle-in-cell/Monte Carlo (PIC/MCC) and Direct Simulation Monte Carlo (DSMC) algorithms. Thruster performance is investigated by permuting electrode geometry (0.5 - 2 cm), chamber pressure (0.05 - 50 Torr), applied voltage (100 - 500 V), and frequency (10 - 1000 MHz). For this parameter space, PIC/MCC determines overall trends in plasma characteristics. One selected case (3 Torr, 500 V, 200 MHz) and its set of conditions (plasma density, plasma heating, gas temperature, etc.) form the basis for an in-depth flow field and thrust performance analysis with DSMC. Assuming adiabatic wall conditions, the RF plasma thruster achieves a specific impulse of 104.4 s with Argon at the throat Reynolds number of 25. The RF heating increases the specific impulse by 125 %. This study shows that propulsive capability of the RF plasma thruster can be enhanced by increasing the discharge chamber length, redesigning the nozzle contour, and using propellants with lower molecular weights.

Nomenclature

d_{gap}	-	gap length of discharge, m
$\frac{E}{n}$	-	reduced electric field, $V \cdot m^2$
$\vec{E}$	-	electric field, $\frac{V}{m}$
f	-	applied RF frequency, Hz
j	-	current density, $\frac{A}{m^2}$
k	-	thermal conductivity, $\frac{W}{m \cdot K}$
n	-	neutral number density, $\frac{1}{m^3}$
nc	-	number of computational cells
n_i	-	ion number density, $\frac{1}{m^3}$

[*]Ph.D. Candidate, E-mail: steinw@purdue.edu, AIAA Student Member.
[†]Assistant Professor, E-mail: alexeenk@purdue.edu, AIAA Member
[‡]Assistant Professor, E-mail: ihrbud@purdue.edu, AIAA Member
[§]Research Scientist, E-mail: bond@itam.nsc.ru, AIAA Member.

$nc2p$	-	ratio of the number of physical particles to computational Particles
p	-	pressure, $Torr$
PLC	-	power loss to collisions, W
PLW	-	power loss to walls, W
T	-	temperature, K
α	-	viscosity-temperature exponent
η_{PC}	-	ratio of power loss to collisions to total power loss
λ_{DE}	-	Debye length, m
Δt	-	time-step, s
ϕ	-	applied potential, V
ν_m	-	electron-neutral collision frequency, $\frac{1}{s}$
ω_f	-	angular applied RF frequency, $\frac{1}{s}$
ω_p	-	plasma frequency, $\frac{1}{s}$

I. Introduction

In the last decade, government agencies, military and industry have recognized the need to deploy small satellites and spacecraft. Key attributes of such spacecraft, which dictate design, are modularity, maneuverability, maintainability, lifetime, autonomous operation and launch/hardware cost.[1] As the size of a spacecraft is reduced, the propulsion wet mass tends to become a more significant portion of the overall system mass. Chemical and electric propulsion alike have to address and deliver propulsive capability within constrains of a mission.[2] In particular, electric propulsion systems have to take into account severe power limitation, which is an inherent characteristic of these proposed spacecraft. Integration of electric microthrusters exceedingly relies on reducing the required power to an absolute minimum, while ensuring reliable, long-term performance.

Since the 1990s, electric propulsion (EP) has been a vital part of spacecraft propulsion for a wide spectrum of space missions and applications for both industry and government agencies. EP provides significant performance benefits compared to cold gas and conventional chemical systems. Commercial satellite manufacturers have embraced EP due to significant economic advantages. To date, electrothermal (arc- and resistojet), electrostatic (Hall and ion thruster) or electromagnetic (pulsed plasma thruster) systems propel close to 200 spacecraft in various mission scenarios spanning lower earth orbit (LEO), geo stationary/synchronous orbit (GST/GSO), and trajectories within the inner planets.[3] However, these applications employ electric thrusters which function best at power levels greater than 1 kW.

In general, microsatellites draw power from solar arrays or batteries to cover their energy need. The main power bus typically operates well below 100 V and, depending on the spacecraft, might deliver power levels up to 100 W. State-of-the-art micropropulsion systems are based on electrostatic acceleration mechanisms, namely FEEP,[4] colloid,[5] ion,[6] and Hall[7] thrusters. Other successful systems encompass micro pulsed plasma thrusters (PPT) and vacuum arc thrusters (VAT).[8,9] These micro propulsion systems require high operating (hundreds to thousands of volts) voltages, all of which exceed typical voltage ceilings for microspacecraft. Power processing units (PPU) must provide significant voltage conversion between the main bus and the microthruster to enable its operating requirements. Extremely high potential differences are present on the microspacecraft at all times increasing the risk of undesirable discharges, which can lead to destruction of sensitive science/mission instrumentation or compromise the propulsion subsystem. Further, these high voltage requirements of most microthrusters preclude a direct-drive scheme, which could reduce power processing to an absolute minimum. Undoubtedly, electric micropropulsion systems afford significantly higher specific impulse over chemical propulsion, thus yielding a substantial reduction in the propulsion system wet mass. It is important that the thruster's power subsystem does not outweigh this benefit. The power supply for an electric thruster is the largest contributor to the propulsion subsystem with regard to mass and volume. On average, the power supply is two to three times more massive than the thruster. As much as microsatellites are power-limited, they also pose significant mass limitations.

As with any system and technology, lifetime issues must be carefully considered. Microthrusters must endure extreme operating conditions and environments making extended lifetime tests an integral part of technology development. In any application where high voltages are involved, electric breakdown properties of dielectrics play a key role. In most of these micropropulsion systems, characteristic dimensions are prone to intensify breakdown/lifetime issues (e.g. breakdown strength).[10] Furthermore, erosion of accelerator electrodes commonly used in colloid and FEEP type propulsion systems is a significant factor due to basic operating principles. High voltage and ions are a precarious combination for erosion and sputtering. Other lifetime limiting issues are back-sputtered particles/secondary electron impingement on emitter tip, diminished insulator properties due to propellant condensation between electrodes, and electron impingement from neutralizer causing overheating and high cesium evaporation.[11]

In this paper we consider an alternative micropropulsion concept, namely, the capacitively coupled RF discharge between coaxial electrodes. This RF plasma thruster is classified as an electrothermal system and has a potential to overcome the severe microsatellite constraints on power, mass, volume, and lifetime. A glow discharge between coaxial electrodes provides heating of a propellant, and thermodynamic expansion of the hot gas generates thrust. In general, glow discharge is characterized as a low-power discharge possessing a low-current density with high uniformity and propagating through low-pressure gas.

The RF discharges have been studied extensively for a variety of applications over the past decades and there is a vast body of literature available regarding theory, modeling and plasma characteristics.[12–14] Preliminary proof-of-concept experiments on RF discharge application for propulsion explored electrode wear by comparing DC and RF operation at comparable levels of power, mass flow rate, and electrode separation. The RF mode showed favorable results with respect to surface condition and discharge stability.[15] Propulsive capabilities of this concept rely on macroscopic parameters such as geometry (electrode separation), mass flow rate (propellant and pressure resulting in heating chamber), frequency (1 MHz to 1GHz), and power. These parameters will be strong determining factors on plasma formation and plasma characteristics, which ultimately will affect heating, erosion, and particle acceleration.

The main goals of this investigation is to develop an efficient computational approach for modeling RF discharge and apply it to simulations of a CCD plasma thruster for various parameters, namely electrode geometry, mass flow rate, peak voltage and frequency. This paper summarizes results of computational modeling which applies PIC and DSMC simulations.

II. Theory

The RF thruster design is based on a capacitively coupled discharge of a gas between coaxial electrodes. The electron and ion motion in the gas discharge is governed by the applied electric potential and momentum transfer due to elastic and inelastic collisions with neutral gas molecules. Coulomb collisions between ions and electrons can be neglected for an RF discharge thruster of this design due to a weak ionization, typically $\frac{n_i}{n} < 10^{-3}$. The oscillations of ions and electrons in a gas discharge are due to a combined effect of two processes, namely - the drift of charges in an electric field and momentum transfer due to collisions. The frequency of such oscillations depends on the effective collision frequency of momentum transfer, ν_m, between charged particles and gas neutrals, and the frequency of the applied frequency. The ratio between the two frequencies is thus a non-dimensional number that characterizes the regime of plasma oscillations. In a limiting case, when $\frac{\omega_f}{\nu_m} << 1$, the plasma can be described as a collisional, continuum media governed by the electrohydrodynamic equations, while for $\frac{\omega_f}{\nu_m} >> 1$, the ions and electrons undergo free oscillations in a collisionless manner which can be described by ballistic-type models. In the transitional regime from the continuum to collisionless plasmas, a kinetic description based on the distribution function of charges is required.

For argon at room temperature, the effective frequency of momentum transfer due to collisions is estimated as[16]

$$\nu_m = 5.3 \times 10^9 P[s^{-1}] \tag{1}$$

Figure 1 shows the collisional regimes of argon discharge as a function of gas pressure and applied voltage frequency. For pressures larger than 10 Torr, the plasma lends itself to a continuum description for frequencies up to 1 GHz. On the other hand, for pressures below 10 Torr, the discharge is in non-continuum regime for the whole RF frequency range. Therefore, to accurately predict argon discharge characteristics at low and moderate pressures that are typical for mN-range thrusters, this study applies a kinetic approach to plasma modeling based on particle-in-cells method with Monte Carlo collisions (PIC/MCC).

III. Modeling Approach

The modeling approach combined both PIC and DSMCC methods for performance analysis of RF plasma thruster. To address the nature of small satellite applications the control parameters encompass pressure, electrode size, frequency and power input. This investigation considers electric power delivered at frequencies of 10 to 100MHz and voltages between 100 and 500 V. The pressure in the discharge chamber varies between 0.05 to 50 Torr. The geometric design of the thruster corresponds to prototypes studied experimentally at Purdue and is shown schematically in Figure 2. The thruster discharge chamber is bounded by coaxial electrodes that is attached to a converging Lexan nozzle with a 2 mm diameter orifice. The PIC plasma simulations are applied for the discharge chamber with a successive DSMC simulations of the propellant expansion through the orifice into vacuum conditions.

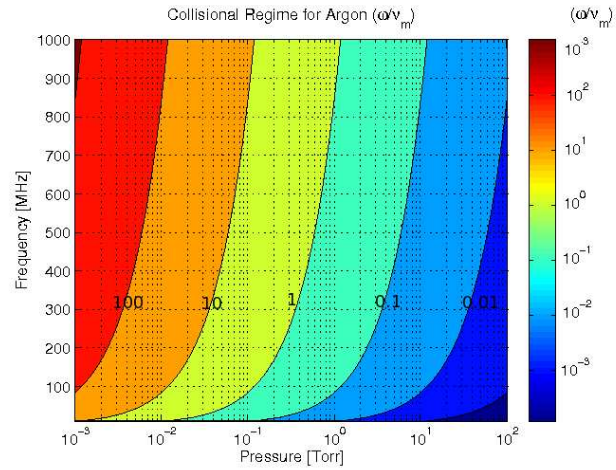

Figure 1. Collisional Regimes for Ar as a function of frequency and pressure

A. PIC/MCC Modeling

The Particle-In-Cell/Monte Carlo Collision (PIC/MCC)[17] method is currently the most powerful approach for kinetic plasma modeling in the collisional regime. PIC/MCC simulations are used to determine plasma characteristics within the coaxial discharge chamber. The charged test particles in PIC/MCC method move in the electric field and representative collisions between charged and neutral particles are calculated using Monte Carlo method. Our model utilizes *XPDC1*, a one dimensional, bounded, cylindrical plasma simulation code developed by the Plasma Theory and Simulation Group at the University of California at Berkeley. Argon collisional model employed in *XPDC1* includes electron-neutral ionization, lumped excitation and elastic scattering using Lawler-Kortsghagen cross-sections.[18] The ion-neutral charge exchange and elastic scattering are also incorporated.[19] The computational parameters of PIC model were chosen to meet the criteria specified below for numerical accuracy:

- Number of Cells: $nc \geq \frac{2d_{gap}}{\lambda_{DE}}$
- Time-step: $\Delta t \leq \frac{0.2}{\omega_p}$ -and- $\Delta t \leq \frac{1}{\omega_f}$
- Ratio of Physical Particles to Computational Particles: $nc2p \approx$ 50-100 computational particles per cell at steady state

The neutral gas temperature is then calculated based on period-averaged electric field and current density by solving the heat conduction equation in the co-axial electrode gap[20]

$$-\frac{1}{r}\frac{\partial}{\partial r}\left[rk\frac{\partial T}{\partial r}\right] = < j \cdot E > \tag{2}$$

subject to the boundary conditions of fixed temperature at the inner and outer electrodes. Here T is the gas temperature, k is the thermal conductivity, j is the electric current density and E is the electric field. The angle brackets on the right-hand side denote period-averaged quantities.

B. DSMC Modeling

The Direct simulation Monte Carlo (DSMC) method is applied to model the neutral gas expansion in the region from the RF discharge annulus to the vacuum chamber. A kinetic approach to modeling neutral gas flow in the thruster is needed due to significant effects of rarefaction in the operating pressure range (mTorr - Torr). The value of the Knudsen number based on the orifice radius of 1 mm is about 0.04 at p=1 Torr and $T = 300$ K. The axisymmetric DSMC code *SMILE*[21] is applied with variable-hard-sphere model, molecular diameter of $d = 4.17 \times 10^{-10}$ m and the viscosity-temperature exponent $\alpha = 0.31$ for argon. Finally, the RF thruster performance parameters such as thrust, mass flow rate and specific impulse are calculated based on the DSMC solution at the orifice exit plane and compared with that for cold gas expansion for the same geometry and pressure.

IV. Results and Discussion

A. Scope of Analysis

The primary goal of this investigation is to discover overall trends regarding RFCCD thruster performance. Ultimately, thrust, specific impulse, and power consumption/power conversion efficiency govern thruster performance. These variables provide a means of performance comparison upon completion of the analysis, but other metrics may be used at earlier stages to evaluate performance as well. Mainly, the ionization rate and power losses provide information regarding how a thruster may perform at various input conditions. This investigation also utilizes four input variables to specify a range of conditions: chamber pressure, inner radius, applied frequency, and applied voltage. The outer electrode radius, and thus the thruster geometry, is defined such that the thruster impedance (in vacuo) is approximately 50Ω. Unless otherwise stated, the inner electrode is fixed at 0.5 cm to represent an existing thruster that is being studied experimentally. Geometry effects such as the inner electrode radius are also investigated in the initial feasibility study. The neutral pressure, applied frequency, and applied voltage vary over a wide range in this initial feasibility stage of analysis.

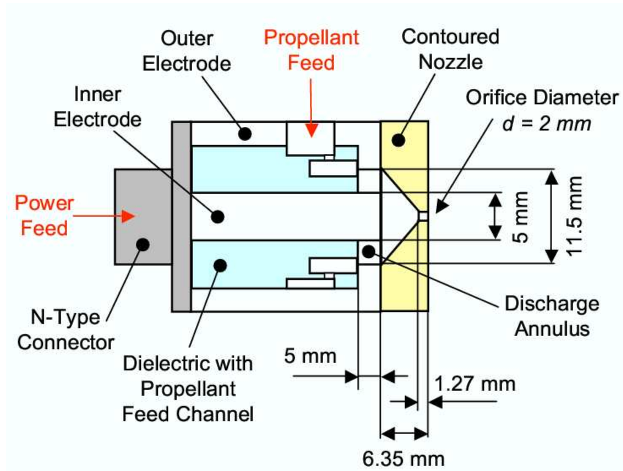

Figure 2. Thruster Schematic

Performance analysis of RF discharge thruster is comprised of three major steps. It begins with the initial feasibility study over a wide range of design variables. This analysis provides general trends for the dependence of ionization rate and plasma heating of neutrals. This is used to refine the discharge parameter space[a] to a region that is more favorable for plasma heating. A refined analysis provides a more detailed and accurate discharge characteristics over the preferred region. Overall ionization rate and the power lost to collisions (PLC) determine the scope of this refined analysis for which steady state results are acquired. From these results a preferred case is chosen and used for the DSMC analysis of the overall thruster performance.

Since this investigation includes a wide range of conditions, some of which being unfavorable for thruster operation, criteria are established *a priori* to determine if the thruster is "operating." A thruster is considered operating when there the plasma number densities stabilize and ionization is present. This investigation considers two types of power loss; that lost to collisions and that lost to electrode impact. Two primary loss mechanisms, thermal and photonic, constitute collisional losses. Unfortunately, there is no present way to separate the two mechanisms, but it is believed that photonic power losses are lower than that of any thermal losses, especially in regions with high values of PLC.

The RF thruster performance is characterized chiefly by its ability to convert the applied electrical power into an efficient means of heating the fluid. This ability can be characterized through a ratio of collisional power loss to the total absorbed power, η_{PC}. This becomes an illustration of how well a given thruster design heats the working fluid for a given amount of total power absorbed by a thruster. This also may provide a metric for evaluating electrode erosion. While particle collisions with the electrodes cannot be totally eliminated in general, conditions may be sought to effectively minimize power loss to the electrodes.

This analysis must also consider limitations in applied power. The PIC/MCC code incorporates either a voltage-limited or current-limited source and does not include any type of power limitation. This poses a problem since the applied power will be physically limited by the type of power supply that is ultimately employed. For the scope of this analysis the power will be limited to an appropriate value set by what is

[a]pressure, voltage, frequency,geometry

deemed realistic for a thruster of this design and mission. This analysis limits the thruster's total absorbed power to approximately 50 W. This limitation effectively filters the available working cases into a subset which matches the desired power requirements. Cases that exceed 50 W are not considered acceptable since a thruster operating at these conditions will require more power than is available. Only cases which have a total power absorption of $50 \pm 10\% W$ are considered desirable.

B. PIC: Initial Feasibility Study

The initial feasibility study investigates general performance trends over 2,304 different sets of operating conditions and further defines a region for additional analysis. Table 1 illustrates the conditions that the initial feasibility study investigated.

Table 1. Parameter Space for Initial Feasibility Study

Variable	Value Range
Pressure [Torr]	0.05 - 50
Inner Electrode Radius [cm]	0.5, 1, 2
Applied Frequency [MHz]	10-1000
Applied Potential [V]	100, 250, 500
Number of Cells	1000
Δt [s]	1e-12
Total Number of Cases	2304

The data shown in Figures 3 and 4 illustrate overall trends demonstrated by this study, primarily a direct correlation between ionization rate and PLC. An increase in the amount of available ions will consequently increase the number of plasma-neutral collisions within the fluid, thus increasing PLC. Figures 3 and 4 also show that an increase in the applied voltage increases the amount of ionization present within the fluid and consequently the amount of power transmitted via collisions. This is expected given that for the same neutral pressure, an increase in the applied voltage increases the reduced electric field, $\frac{E}{n}$, the ratio of the electric field to the neutral gas number density. This increase in $\frac{E}{n}$ can also be seen as an increase in the amount of available kinetic energy between neutral collisions and improves particle ionization. Further, the results of this analysis demonstrate the requirement of a minimum value of reduced electric field for ionization and thruster operation. This minimum represents a lower bound of the energy available for ionization. For conditions where $\frac{E}{n}$ produces inadequate ionization, the plasma becomes unsustained. This effect occurs in two regions: at a low applied voltage and consequently a low electric field, or at a higher pressure. Thus, ionization rate and PLC are bounded both by conditions where the applied voltage is low for a given pressure and the pressure is high for a given voltage.

In the frequency/pressure domain, pressure determines the number of plasma-neutral collisions available for energy exchange, while frequency designates how fast the plasma may oscillate through the fluid. These low collision rates bound performance at lower pressures while performance at higher pressures is bounded by insufficient values of $\frac{E}{n}$. While there may be sufficient energy for ionization at lower pressures, the number of collisions is too small and thus, the magnitude of the power absorbed via collisions is small compared to conditions at higher pressures. At higher frequencies, the oscillation amplitude is insufficient to provide enough neutral collisions such that ionization can sustain the plasma.

When looking at how the inner electrode radius and thus thruster geometry affects performance, two competing mechanisms arise. First, as the radius of the electrodes increases so does the electrode separation. This decreases the electric field for a given applied potential via $\vec{E} = \frac{\partial \phi}{\partial r}$. This lowered electric field weakens the reduced electric field and thus the effectiveness of the thruster to ionize neutrals efficiently. While this may seem to be detrimental to thruster performance, an increase in radius increases the available volume and consequently the number of ions within the chamber at a given pressure. These two competing effects limit the thruster geometry. For a given voltage and pressure, if the thruster is too small there will be insufficient ionization to sustain the plasma regardless of the magnitude of the electric field because the ionization rate will be less than any diffusive losses. If a thruster becomes too large, the electric field will be too weak to effectively ionize the fluid despite the neutral number density. These competing effects bound the thruster size and hence an optimum thruster size exists for a given pressure and voltage. This investigation resides

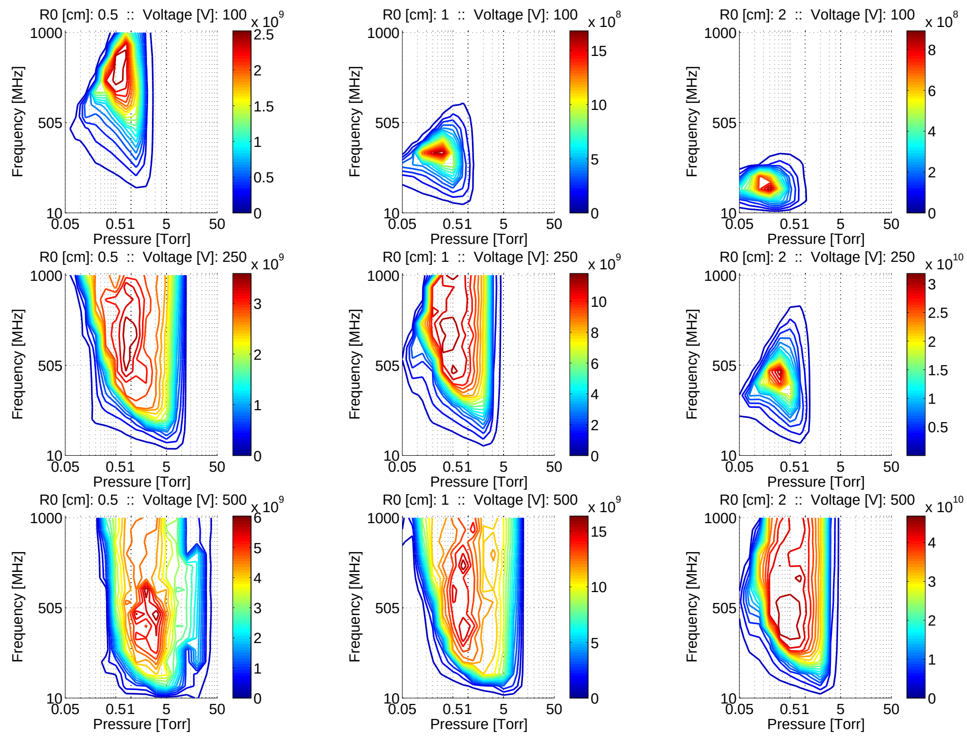

Figure 3. Ionization rate as a function of pressure, frequency and voltage.

near the lower/minimum radii boundary. Figures 3 and 4 illustrate this point, given that the ionization rate decreases as the inner radius decreases. This investigation did not find an upper limit for thruster size.

C. PIC: Refined Analysis

The data from the initial feasibility study suggests regions of thruster feasibility. Because conditions of the initial feasibility study have not reached a steady state, their overall numbers are not truly indicative of thruster performance. What is apparent is how a thruster will perform at each set of conditions. Regions of high ionization, while constructive, may transition into a more arc-like discharge which becomes detrimental to electrode lifetime. The refined analysis region consists of 100 cases determined by the region where the total absorbed power is less than 100 W, but is in a region where steady state results would dictate conditions conducive to thruster performance of approximately 50 W. Table 2 below prescribes the region of refined analysis.

Table 2. Parameter Range for Refined Analysis

Variable	Value Range
Pressure [Torr]	1-3
Inner Electrode Radius [cm]	0.5
Applied Frequency [MHz]	100-250
Applied Potential [V]	500
Number of Cells	1000
Δt [s]	1e-12
Total Number of Cases	100

Refined analysis shows two major trends. Within this region shown in Figure 5, total power consumption increases with both pressure and applied frequency. Dividing the total power consumption into components regarding fluid collisions and losses to the electrodes, an increase in pressure increases PLC but decreases

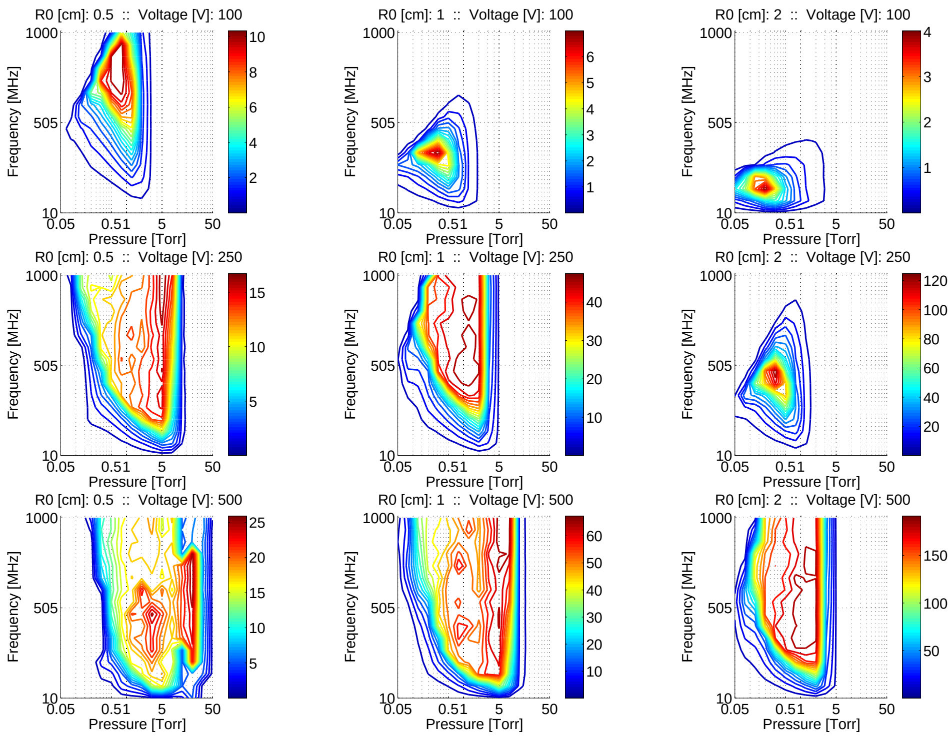

Figure 4. Power lost to collisions as a function of pressure, frequency and voltage.

the power lost to the walls (PLW). Increasing the applied frequency also increases PLC, but has a lesser effect on PLW.

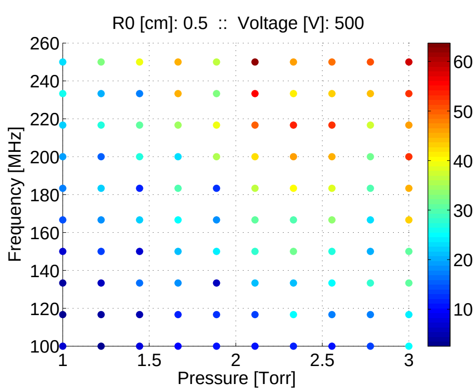

(a) TPL [W]

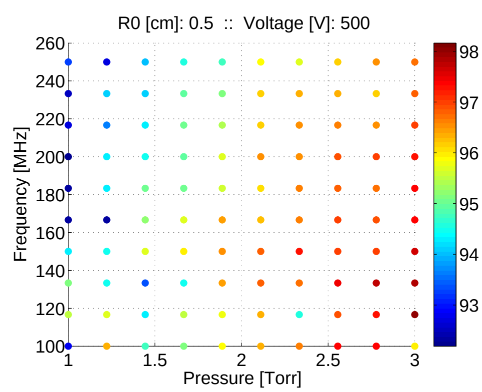

(b) η_{PC}

Figure 5. Refined Analysis: Results

D. PIC: Favorable Discharge Conditions

Results from the refined analysis indicate that the power requirements may be satisfied over a range of conditions, primarily this region being isolated between 2-3 Torr and 200-250 MHz. These conditions are listed in Table 3.

Table 3. Set of Conditions meeting Power Requirements ($50W \pm 10\%$ 0.5 cm, 500 V)

Pressure [Torr]	Applied Frequency [MHz]	PLC [W]	PLW [W]	η_{PC}
2.11	216.67	48.99	1.88	0.96
2.11	233.33	54.52	2.10	0.96
2.33	200.00	46.09	1.59	0.97
2.33	216.67	53.01	1.87	0.97
2.33	250.00	45.24	1.97	0.96
2.56	216.67	52.08	1.73	0.97
2.56	250.00	48.35	1.88	0.96
2.78	250.00	50.35	1.76	0.97
3.00	**200.00**	**52.24**	**1.39**	**0.97**
3.00	216.67	45.50	1.36	0.96
3.00	233.33	52.68	1.66	0.97

While there is some variance between PLC and PLW values in general, there is little change in η_{PC}. This invariance of η_{PC} within this region makes it difficult to find only one preferred case to be used in further analysis. The case in bold type in Table 3 are the set of conditions that are favorable in terms of having a relatively high PLC, a high η_{PC}, and the highest chamber pressure. Since this case lies along a boundary of the refined analysis data, a better choice of conditions may occur outside this analysis region. This is left to future investigations and thruster performance optimization. The final distribution of ions and neutral temperature for this case were used in the DSMC simulations and are plotted in Figure 6. One limitation of the PIC/MCC model is the assumption of no thermal transport between the plasma and neutrals. This is a poor assumption, since the main goal of thruster operation is to heat the working fluid and increasing the neutral temperature decreases the neutral number density. The DSMC code used for the final case study incorporates changes in the neutral temperature to provide a more realistic thruster model, but power absorption will be lower than the stated values used in this analysis. Future versions of this model will employ methods to incorporate changes in temperature directly into the PIC/MCC analysis.

E. DSMC: Flow Structure and Performance

The DSMC modeling was applied to obtain the flowfields and thrust performance of the RF plasma thruster for a pressure of 3 Torr an applied voltage of 500 V and RF frequency of 200 MHz. The DSMC computational domain was bounded by the exit of the discharge chamber at left ($x = 0$), see Figure 2, the converging nozzle wall and the vacuum chamber as the outflow boundary. The inflow boundary at the discharge chamber exit corresponded to a constant pressure of 3 Torr, zero velocity and gas temperature profile obtained via PIC plasma simulations (Fig. 6(c)). The cold gas expansion with stagnation temperature of 300 K and a pressure of 3 Torr for the same thruster geometry was calculated for RF thruster performance comparison. The main mechanism for performance gain is through the plasma heating of propellant gas obtained by an RF discharge. The performance of such electrothermal propulsion system is affected by heat transfer losses to the nozzle walls. The effect of heat losses was investigated by considering two different thermal conditions at the nozzle wall boundary. The case of adiabatic nozzle wall is modeled using zero energy accommodation coefficient in the Maxwell gas-surface interaction model. Another case considered of a cold nozzle wall with a constant temperature of 300 K. The calculated X-velocity profiles for the three cases are shown in Fig. 7(a). The X-velocity at the nozzle exit is about 220 m/s for the cold gas case, whereas for the RF discharge conditions the axial velocities are 530 m/s for adiabatic and 280 m/s for constant wall conditions. The influence of the nozzle wall thermal boundary conditions on the RF discharge thruster is illustrated in Fig. 7(b) where the argon gas temperature contours are plotted for adiabatic (top) and cold wall conditions (bottom). The temperature at the thruster exit is about 1,200 K, the temperature is about 530 K for the cold nozzle wall. Therefore, the heat losses to the nozzle wall has a major effect on RF thruster performance. The calculated thrust, mass flow rate and specific impulse for the three cases are listed in Table 4. The thrust levels in all three cases are very close, whereas the mass flow rate is significantly smaller in the RF discharge cases compared to the cold gas nozzle. This is due to the lower mass density at the same stagnation

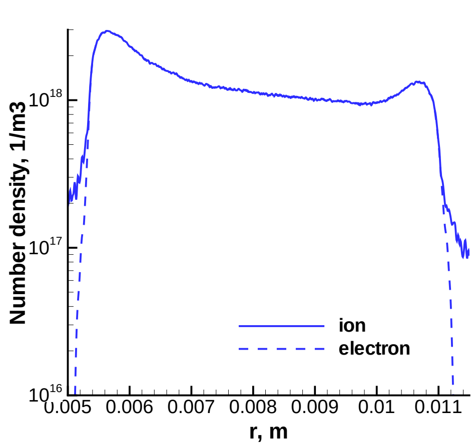

(a) Plasma Density

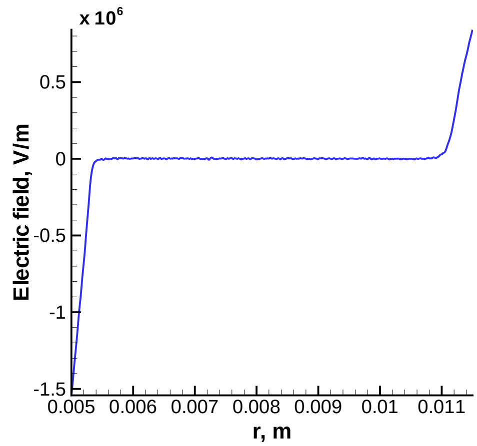

(b) Time-Averaged Electric Field

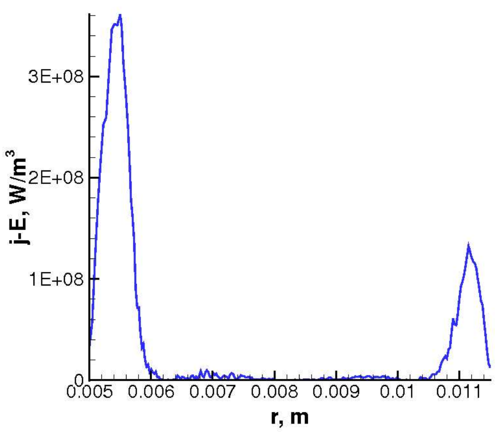

(c) Plasma heating $j \cdot \vec{E}$

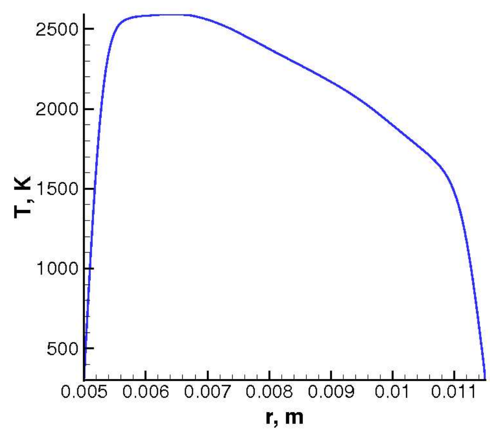

(d) Gas Temperature

Figure 6. Radial Distributions Calculated by PIC for the Favorable Discharge Conditions

Table 4. RF thruster performance at pressure of 3 Torr, applied voltage of 500 V and RF frequency of 200 MHz)

Case	Thrust, mN	Mass flow rate, kg/s	Specific impulse, s
RF Discharge (adiabatic wall)	1.31	1.28	104.4
RF Discharge (300 K wall)	1.37	2.25	61.9
Cold gas	1.40	3.08	46.4

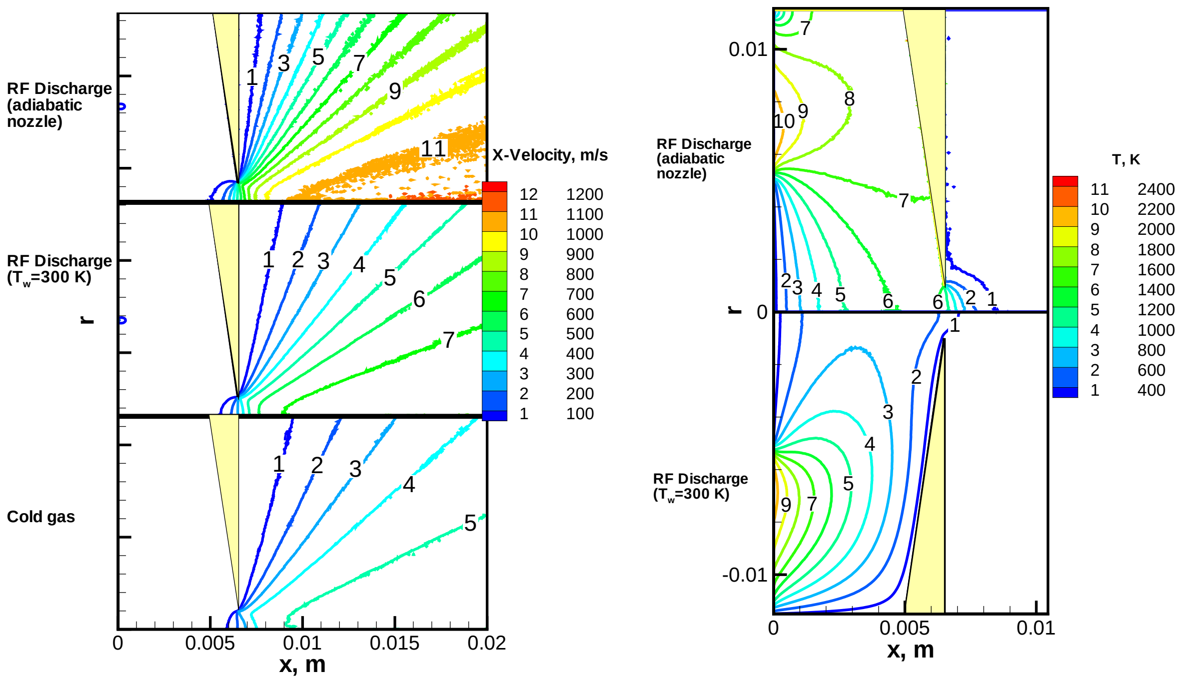

(a) X-Velocity Contours

(b) Temperature Contours

Figure 7. DSMC calculated flowfield for a pressure of 3 Torr

pressure. The specific impulse for RF discharge with adiabatic wall is more than two times larger than that for a cold gas.

There are several ways to further increase the specific impulse of such a RF plasma thruster. First, a propellant that is easy to ionize and that has a lower molecular weight, e.g., helium would allow an increase the specific impulse by factor of approximately two. Second, the discharge at higher pressure would decrease viscous losses and allow to achieve a supersonic flow if a converging-diverging nozzle is used. For the current thruster configuration and discharge pressure of 3 Torr, the Reynolds number at the orifice plane is about 25. At such a low Reynolds number, viscous losses are extremely large and the efficiency of converging-diverging nozzle is even lower than that of an orifice expansion.[22] The experimental and numerical results[22] for gas expansion through nozzles and orifices at low Reynolds numbers indicate that in order to achieve a supersonic flow the pressure has to be increased by a factor of about 10. RF glow discharge at such high pressures can be achieved for millimeter-scale coaxial gaps, if the discharge chamber length increases. If these two mechanisms for increasing the specific impulse of RF plasma thruster are applied, the specific impulse of such an electrothermal micropropulsion system can approach that of macroscale chemical thrusters.

V. Conclusions

An RFCCD thruster was successfully modeled using a combination of PIC and DSMC simulations. It has been demonstrated that there is a required minimum applied potential such that electrons gain enough kinetic energy within a single oscillation for sustainable ionization to occur. These oscillations must also have a sufficient amplitude for a given pressure such that the electrons collide with enough neutrals and provide ionization rate large enough to sustain a glow discharge. In addition, there exists an optimum thruster geometry prescribed by the radius of the inner electrode for a given set of conditions in terms of power input and impedance. This is governed by requirements in reduced electric field and plasma number densities. Thrust and specific impulse for a argon RF discharge thruster operating at the favorable conditions for propellant heating have been calculated. It has been shown that the RF discharge thruster can provide more than a two-fold increase in specific impulse as compared to a cold gas thruster operating at the same pressure and geometry. The results of this study will provide a baseline for future work on RF plasma thruster optimization in terms of discharge chamber size, propellant selection and operating pressures. These modeling shows that RF plasma discharge concept can potentially provide thrust in the milli-Newton range while meeting stringent power and size limitations and achieving specific impulse comparable to larger scale chemical propulsion systems.

Acknowledgments

Our research group would like to thank Dr. J.P. Verboncoeur, Dr. C.K. Birdsall and the Berkeley Plasma Theory and Simulation Group for the use of their *XPDC1* code and providing assistance. We would also like to thank Dr. Mikhail Shneider for extremely valuable discussions of RF discharge physics.

References

[1]C. Sultan, S. S. and Mehra, R., "Deep Space Formation Flying Spacecraft Path Planning," *International Journal of Robotics Research*, 2007.

[2]Myers, R., "Small Satellite Propulsion Options," *NASA TM 106701*, 1994.

[3]Myers, R., "Overview of Major U.S. Industrial Electric Propulsion Programs," *40th AIAA Joint Propulsion Conference and Exhibit*, 2004, AIAA 2004-3331.

[4]Ziemer, J. and Merkowitz, S., "Microthrust Propulsion for the LISA Mission," *40th AIAA Joint Propulsion Conference*.

[5]et al., M. H., "Micro-Newton Colloid Thruster for ST7-DRS Mission," *39th AIAA Joint Propulsion Conference*.

[6]R. Wirz, M. G. and Mueller, J., "Miniature Ion Thrusters for Precision Formation Flying," *40th AIAA Joint Propulsion Conference*.

[7]Warner, N. and Martinez-Sanchez, M., "Design and Preliminary Testing of a Miniaturized TAL Hall Thruster," *42nd AIAA Joint Propulsion Conference*.

[8]C. Rayburn, M. Campbell, W. H. and R., "Development of a Micro Pulsed Plasma Thruster for the Dawgstar Nanosatellite," *39th AIAA Joint Propulsion Conference*.

[9]et al., M. A., "Magnetically Enhanced Vacuum Arc Thruster (MVAT)," *40th AIAA Joint Propulsion Conference*.

[10]Mueller, J., "Microfabricated Ion Accelerator Grid Design Issues: Electric Breakdown Characteristics of Silicon Dioxide Insulator Material," *34th AIAA Joint Propulsion Conference*, 1998, AIAA 98-3923.

[11]S. Marcuccio, A. G. and Andrenucci, M., "FEEP Microthruster Technology Status and potential Applications," *48th International Astronautical Federation Congress*, 1997, IAF-97-S.3.04.

[12]Lieberman, M. and Lichtenberg, A., *Principles of Plasma Discharges and Materials Processing*, John Wiley and Sons, 1994.

[13]Godyak, V., *Soviet Radio Discharge Research*, Delphic Associates, Inc., 1986.

[14]Y.P. Raizer, M. S. and Yatsenko, N., *Radio Frequency Capacitive Discharges*, CRC Press, 1995.

[15]Hrbud, I., "RF Plasma Thruster for SmallSat Applications," *35th AIAA Joint Propulsion Conference*, July 1999.

[16]Raizer, Y., *Gas Discharge Physics*, Springer-Verlag, 1991.

[17]Birdsall, C. and Langdon, A., *Plasma Physics via Computer Simulation*, McGraw-Hill, 1985.

[18]Lawler, J. and Kortshagen, U., "Self-consistent Monte Carlo simulations of the positive column of gas discharges," *Phys D: Appl Phys*, Vol. 32, 1999, pp. 3188–3198.

[19]*Cylindrical Plasma Device 1-D Bounded Electrostatic Code*, Plasma Theory and Simulation Group, University of California, Berkeley.

[20]Raizer, Y. P. and Shneider, M., "Coaxial Medium-Pressure RF Discharge: Dynamics of Plasma Oscillations," *Plasma Physics Reports*, Vol. 21, No. 3, 1995, pp. 260–267.

[21]Ivanov, M., Markelov, G., and Gimelshein, S., "Statistical Simulation of Reactive Rarefied Flows: Numerical Approach and Applications," *AIAA Paper 98-2669*, 1998.

[22]Ketsdever, A., Clarbough, M., Gimelshein, S., and Alexeenko, A., "Experimental and Numerical Determination of Micropropulsion Device Efficiencies at Low Reynolds Numbers," *J. of AIAA*, Vol. 43, 2005, pp. 633–641.